Title: Genetic modification of the bee parasite *Crithidia bombi* for improved visualization and protein localization

Blyssalyn V. Bieber*[1], Sarah G. Lockett*[1], Sonja K. Glasser[2], Faith A. St. Clair[1], Neida O. Portillo[2], Lynn S. Adler[2], Megan L. Povelones¶[1]

*co-first authors
¶corresponding author

[1]Department of Biology, Villanova University, Villanova, PA 19085 USA
[2]Department of Biology, University of Massachusetts Amherst, Amherst, MA 01003 USA

Corresponding Author: Megan Povelones, Villanova University
megan.povelones@villanova.edu

ORCID:
Blyssalyn V. Bieber: 0009-0007-2771-8791
Sarah G. Lockett: 0009-0009-4751-8505
Sonja K. Glasser: 0000-0001-6733-8610
Faith A. St. Clair: 0009-0001-9794-9233
Neida O. Portillo: 0000-0003-3480-5336
Lynn S. Adler: 0000-0003-2125-5582
Megan L. Povelones: 0000-0003-2612-6413

Abstract

Crithidia bombi is a trypanosomatid parasite that infects several species of bumble bees (*Bombus* spp.), by adhering to their intestinal tract. *Crithidia bombi* infection impairs learning and reduces survival of workers and the fitness of overwintering queens. Although there is extensive research on the ecology of this host-pathogen system, we understand far less about the mechanisms that mediate internal infection dynamics. *Crithidia bombi* infects hosts by attaching to the hindgut via the flagellum, and one previous study found that a nectar secondary compound removed the flagellum, preventing attachment. However, approaches that allow more detailed observation of parasite attachment and growth would allow us to better understand factors mediating this host-pathogen relationship. We established techniques for genetic manipulation and visualization of cultured *C. bombi.* Using constructs established for *Crithidia fasciculata,* we successfully generated *C. bombi* cells expressing ectopic fluorescent transgenes using two different selectable markers. To our knowledge, this is the first genetic modification of this species. We also introduced constructs that label the mitochondrion and nucleus of the parasite, showing that subcellular targeting signals can function across parasite species to highlight specific organelles. Finally, we visualized fluorescently tagged parasites *in vitro* in both their swimming and attached forms, and *in vivo* in bumble bee (*Bombus impatiens*) hosts. Expanding our cell and molecular toolkit for *C. bombi* will help us better understand how factors such as host diet, immune system, and physiology mediate outcomes of infection by these common parasites.

Keywords

trypanosomatid, kinetoplastid, *Crithidia bombi*, *Bombus impatiens*, nucleofection

Acknowledgments

This work was supported by a National Science Foundation IntBIO award number 2128223 to LSA and MLP. We thank Ben Sadd and Emmanuel Tetaud for advice and reagents, and Koppert Biological and Biobest for discounted or donated bumble bee colonies. *In vivo* microscopy was performed in the Light Microscopy Facility and Nikon Center of Excellence at the Institute for Applied Life Sciences at the University of Massachusetts Amherst with support from the Massachusetts Life Sciences Center. We thank Madeline Malfara along with Lindsay Bair, Laura Anastor-Walters, Gabrielle Schusler, and Nancy Peltier at Villanova University for technical assistance. Many thanks to Dana Opulente, also at Villanova, for help with sequencing and genome analysis.

Introduction

Trypanosomatids of the class Kinetoplastea are single-celled eukaryotic parasites [1]. While some trypanosomatid species, such as *Leishmania*, can be transmitted to humans by insect vectors causing considerable morbidity and mortality [2], most trypanosomatids are monoxenous and exclusively parasitize insects [3]. For these parasites, fecal-oral transmission is the most common mode of pathogen spread [4]. This cycle requires an infected host to defecate parasites onto a food source, where they must remain viable long enough to be ingested by their next susceptible host. Once in the host, parasites often accumulate in the hindgut and rectum, adhering to the lining of these tissues by their single flagellum and dividing by binary fission as attached cells [4]. The structure of this flagellar attachment is similar in all trypanosomatids [5,6].

Some trypanosomatids infect bees such as honey bees (*Apis mellifera*) and bumble bees (*Bombus* spp.), potentially contributing to pollinator decline [7]. For example, *Crithidia bombi* is a gut parasite primarily known to infect multiple species of bumble bees, including *Bombus impatiens* and *Bombus terrestris*, although *C. bombi* has recently been found to replicate in the solitary bee species *Osmia lignaria* and *Megachile rotundata* as well [8]. In bumble bees, *C. bombi* impairs learning [9], can reduce queen colony-founding success [10], and can reduce worker survival under stressful conditions [11]. Other trypanosomatids, such as *Lotmaria passim*, cause similar effects in honey bees [12]. The presence of the parasites triggers an immune response in the bee host, including production of antimicrobial peptides (AMPs), although precisely how infection impacts host fitness is unclear [13,14]. Researchers have also shown that gene expression patterns in cultured parasites differ from those of parasites in the bee gut, representing possible metabolic adaptations to the host environment [14].

Certain floral diets can reduce *C. bombi* infections in some bumble bee species. The secondary metabolite callunene, discovered in the nectar of heather flowers (*Calluna vulgaris*), removed or shortened the flagellum of *C. bombi* and dramatically reduced infection in *B. terrestris,* presumably by interfering with the parasites' ability to adhere to and colonize the gut [15]. Similarly, pollen of sunflower (*Helianthus annuus*) and some other Asteraceae plants dramatically decreases *C. bombi* infection in *B. impatiens* [16–20] but is less effective in other

Bombus species [21], suggesting that species-level variation shapes diet-mediated effects on infection outcomes.

The underlying mechanisms for the antiparasitic effect of different floral products such as pollen and nectar are largely unknown. Molecular genetic tools to manipulate parasites for *in vivo* infections and in culture would facilitate new experimental approaches to understand how floral resources impact host-pathogen dynamics. For instance, which parasite biological processes are disrupted by heather nectar or sunflower pollen? Possible targets include flagellar growth, attachment, and survival and division of attached cells. Discovering the effects of floral products on these activities could improve our understanding of how these different aspects of parasite biology contribute to productive infections. Although all trypanosomatids, including human pathogens, attach to tissues in their insect hosts [6], insect parasites do so in great numbers [4], meaning they could serve as a model for insect colonization by trypanosomatids more generally. In addition, improved understanding of the effects of pollen and nectar diets on the mechanisms underlying parasite infections could allow us to predict the impacts of floral resources on pathogen load and pollinator health.

Detailed study of attachment and modes of cell division would be greatly facilitated by improved visualization of parasites *in vivo*. For this, both whole cell and organelle markers would allow researchers to monitor the number, location, and cellular structure of parasites at different stages of the infection. Such analyses would improve our understanding of the life cycle of these parasites in their insect hosts, which could reveal vulnerabilities for intervention. *In vitro* assays for infection behaviors such as attachment would allow for time-resolved, quantitative studies showing how attachment changes under different conditions, predicting infection dynamics in the presence and absence of different floral products and compounds. Finally, genome-wide transcriptomics and proteomics approaches will reveal gene products that mediate interactions between parasites and their insect hosts [13]. Genetic techniques enabling functional knockout and subcellular localization during the cell and life cycle of the parasite would provide important insights into the mechanism of action of specific proteins.

To develop these approaches, our objectives for this study were to 1) establish *C. bombi* sensitivity to antibiotics used as selectable markers, 2) introduce episomal plasmids including genes for enhanced green fluorescent protein (eGFP) and red fluorescent protein (RFP) into *C. bombi* cells, 3) create markers for subcellular organelles, 4) isolate and culture parasites from *B. impatiens* intestinal tracts, and 5) visualize fluorescently-labelled *C. bombi* cells *in vitro* and *in vivo*.

Methods

Parasite lines and culture

To establish sensitivity to antibiotics, *C. bombi* strains 08.076 and 16.075 (provided by Ben Sadd, Illinois State University) were cultured in FP-FB media supplemented with 2 µg/mL hemin (Sigma, St. Louis, MO) and 10% fetal bovine serum (Atlanta Biologicals, Bio-Techne, Minneapolis, MN) at 27 °C and 3% CO_2, as described [22]. For drug sensitivity tests and maintaining genetically modified parasite lines, medium was supplemented with either

hygromycin (Hyg, catalog number 10687010, ThermoFisher) or neomycin (Neo, G418, catalog number G8168, Sigma). Growth curves were performed in triplicate and drug concentrations ranging from 0 to 80 µg/ml in 2-fold increments were tested. Parasites were grown in sterile, untreated tissue culture plates or 25 cm^3 flasks with vented caps. Cell densities were determined by removing a 25 µL sample of the culture to a 1.5 mL tube, adding 25 µL of 3% formalin to fix, followed by 200 µL of Gentian violet (Harleco) staining solution [23]. 10 µL of this mixture was then applied to a Neubauer hemacytometer and counted on an inverted tissue culture light microscope (Zeiss Primovert). Parasites were maintained between 5 x 10^5 and 5 x 10^7 cells/mL by diluting in fresh medium every 2-3 days. To generate attached parasites, 2 mL of log-phase parasites (1-2 x 10^7 cells/mL) were allowed to adhere to a poly-L-lysine coated dish (MatTek, Ashland, MA) for 24 hours, followed by washing 3X with 1X PBS to remove non-attached cells.

Plasmids and transfection

To introduce plasmids into *C. bombi*, the pNUS series of plasmids containing sequences for expression of transgenes in *Crithidia fasciculata* and *Leishmania* were used (provided by Emmanuel Tetaud) [24]. The pNUS-eGFP-cH (enhanced green fluorescent protein, hygromycin resistance) and pNUS-RFP-cN (red fluorescent protein, neomycin resistance) were transfected unmodified into *C. bombi* strains 08.076, 16.075, or WHA1. For organelle markers, the pNUS-mitoeGFP-cH was created as described [25]. To create pNUS-*Cf*RNH1eGFP-cH, the open reading frame (lacking the stop codon) for the RNase H1 gene from *C. fasciculata* (*Cf*RNH1, TriTrypDB accession number CFAC1_220025400) was amplified by PCR using primers 5'-GCTACTAGCATATGATGAAGCCGTCGTTTTATGTA and 5'-GCTACTAGGGTACCCTCACTGGTCCCGTGCATACG containing NdeI and KpnI restriction enzyme sites, respectively (underlined). The amplified product was cloned into pNUS-eGFP-cH using NdeI and KpnI restriction sites resulting in fusion of eGFP to the C-terminus of *Cf*RNH1. Plasmids were confirmed by Sanger (Eurofins Genomics, Louisville, KY) or Nanopore (Plasmidsaurus) sequencing. Circular plasmids were concentrated by ethanol precipitation and resuspended in sterile water at a concentration of 0.5 µg/µL. For nucleofection, 1 x 10^8 *C. bombi* cells were harvested by centrifugation (5 min, 800 rcf) and resuspended in 100 µL TbBSF buffer [26]. 5 µg of plasmid was added to the tube and the solution was mixed briefly before being transferred to a Lonza cuvette. Parasites were nucleofected using program X-001 on a Lonza Nucleofector 2b device. Cells were then transferred to media and allowed to recover for 24 hours before addition of selecting drug to a final concentration of 40 µg/mL. An equal number of untransfected cells were resuspended in the same drug concentration as a "mock" control for drug effectiveness. After 10 days of selection, surviving cells were screened by fluorescence microscopy. The concentration of the selecting drug was then increased to 80 µg/mL.

Microscopy of cultured parasites

Expression of fluorescent proteins expressed in the cytoplasm or in organelles was detected by fluorescence microscopy. 1 x 10^7 cells were harvested by centrifugation (5 min, 800 rcf) and washed once with PBS. Cells were allowed to adhere to poly-L-lysine coated coverslips for 20 min in a humid chamber at room temperature followed by 2 washes in PBS. Cells were fixed with cold 4% paraformaldehyde for 15 min then washed twice with PBS. Cells were permeabilized in 0.1% Triton X-100 in water for 5 min followed by 2 washes in PBS, stained with 2 µg/mL DAPI (a 2 mg/ml stock prepared in water was diluted to 2 µg/ml in PBS), washed in PBS, and mounted in Vectashield (Vector Laboratories, Burlingame, CA). Parasites were

imaged on a Leica SP8 confocal microscope using the 100x objective. Z-stack images with 0.2 µm steps were taken for all *in vitro* fluorescent cell microscopy. Final images shown in figures are max projections of the z-stack images. Pearson's coefficients for co-localization were calculated used the JACoP plugin in Fiji [27,28]. Attached parasite rosettes were imaged live in PBS.

Episomal stability in cultured cells

For experiments testing the stability of the episomal transgene, the clonal isolate *Cb*-WHA1-RFP was cultured in the presence or absence of the selecting drug neomycin (3 flasks per treatment) for 22 days. Every 2-3 days (9 time points total), a 500 µl sample was removed, centrifuged at 800 rcf for 5 min, and resuspended in 250 µl of filtered Ringer's solution. A 20 µl droplet of this suspension was then added to a microscopy slide and covered with a coverslip. Live cells were promptly imaged using a Nikon TiE microscope equipped with NIS-Elements 5.3 software with an A1R confocal system at 20X magnification in both brightfield and red fluorescence channels. This microscope was also used for *in vivo* imaging described below and is housed in the Light Microscopy Facility and Nikon Center of Excellence at the Institute for Applied Life Sciences at the University of Massachusetts Amherst. At least 100 cells per time point were imaged using brightfield and red fluorescence. The latter was quantified using a NIS-Elements GA3 analysis custom pipeline. The effect of fixed factors (neomycin presence/absence, number of trial days) and their interaction with the proportion of fluorescent to total cells was assessed using a beta distributed mixed model (glmmTMBfunction 'glmmTMB', [29]). The proportion of fluorescent cells:total cells was averaged across images of 4-5 fields of view from each prepared slide. Flask ID was included as a random effect. Collinearity between the predictor variables was assessed (car function 'vif' [30]) and VIF scores were <5 confirming no collinearity between variables. Model fit was validated using QQ and residual plots comparing the simulated residuals with observed residuals (DHARMa functions 'simulateResiduals', 'plot' [31]).

Isolation of parasites from Bombus impatiens

Crithidia bombi (origin, Hadley, Massachusetts: 42.363911 N, −72.567747 W) were collected from the wild in 2014 and thereafter maintained as a live infection in commercial *B. impatiens* colonies (Koppert Biological Systems, Howell, Michigan, USA and Biobest USA Inc., Romulus, Michigan USA). We randomly selected five bees, dissected their digestive tracts, and homogenized the tissue in 300 µL of isotonic Ringer's solution. After three hours, a 150 µL sample was taken from the top of the homogenized solution and centrifuged (5 min, 800 rcf). Pelleted material was resuspended in 5 mL of FP-FB medium and stored at 4 °C. Additionally, feces from five infected bees from the same colony were collected using capillary tubes, transferred directly into 5 mL of FP-FB medium, and stored at 4 °C for up to five days. We modified the protocol established in [22] to isolate *C. bombi* cells from the bee digestive tracts and feces. The samples were centrifuged (5 min, 800 rcf) and resuspended in 1 mL of one of two different modified "Mäser Mix" media. One included 1% antibiotic [Penicillin-Streptomycin (Pen-Strep), Sigma Aldrich] while the other included both 1% Pen-Strep and 1% antifungal, Amphotericin B (250 µg/mL, Sigma Aldrich), both in FP-FB medium. Parasites were incubated at 27 ºC and 3% CO_2 overnight followed by cloning by limiting dilution in 96 well plates at a calculated density of 0.5 cells/well or 0.1 cells/well. Two weeks later, positive clones were identified as containing parasites without bacterial or fungal contaminants and scaled up for further analysis. These 30 clonal isolates were internally named WHA1-WHE6.

PCR and sequencing

To identify our *Crithidia* strains as *C. bombi* rather than the cryptic species *C. expoeki*, total genomic DNA (gDNA) was isolated using the GeneJet Genomic DNA Purification Kit (Thermo catalog number K0721) and was used to amplify *gGAPDH* and *SSU rRNA* genes using the primers described in [32]. To isolate mitochondrial DNA, kinetoplast DNA (kDNA) networks were purified over a 20% sucrose cushion as in [33]. Isolated kDNA was used as the template for PCR reactions amplifying *Cyt B*. PCR products were amplified using Taq polymerase (New England Biolabs catalog number M0273S) according to the manufacturer's protocol. Annealing temperatures for each target were determined empirically (*gGAPDH* 52.7 °C, *SSU rRNA* 61. 2 °C, *Cyt B* 45 °C). Single PCR products for *gGAPDH* and *SSU rRNA* were purified using an exonuclease I/Antarctic phosphatase procedure as in [34]. These targets were sequenced by Sanger sequencing using the forward primer and the BigDye Terminator v3.1 Cycle Sequencing Kit (ThermoFisher catalog number 4337454) followed by sequencing on a SeqStudio Genetic Analyzer (applied BioSystems, ThermoFisher). For *Cyt B*, column-purified (Promega kit) single PCR products were sequenced on both strands at Eurofins Genomics. Sequences were trimmed in Geneious software and aligned to reference sequences (*C. bombi*: GU321192, GU321194, GU321187, GU321188; *C. expoeki*: GU321193, GU321195, GU321189, GU321190) using Clustal Omega [35]. Final formatted alignments were created in Jalview [36].

Laboratory infections of Bombus impatiens

To visualize *C. bombi* infection *in vivo*, inoculum was prepared by sampling from an early log phase culture (6.5×10^5-6.5×10^6 cells/mL) of *C. bombi* strain WHA1 expressing either eGFP or RFP. To remove cells from media containing the selecting drug, cells were centrifuged (5 min, 800 rcf), washed twice with Ringer's Solution, and then resuspended in equal parts Ringer's Solution and 30% sucrose solution (in distilled water) to create a final inoculum of 1200 cells/µL and 15% sucrose solution. *Bombus impatiens* workers were sampled from uninfected colonies (Koppert Biological Systems, Howell, Michigan, USA), transferred to individual vials, starved for 3-4 hours, then presented with two 15 µL droplets of inoculum and observed until both drops were consumed. Only bees that consumed both droplets were included in experimental trials. To allow for the infection to progress, 5-6 bees inoculated with either eGFP or RFP-expressing *C. bombi* infections were placed into deli cups (clear plastic cups with clear lids, 7.62 cm tall, base diameter 9.53 cm, top diameter 11.43 cm, SOLO Cup Company) and fed *ad libitum* on 30% sucrose and wildflower pollen (CC Pollen Company, Phoenix, Arizona, USA). After allowing infections to progress 7 days post-inoculation, we dissected the bees and imaged the digestive tracts using a Nikon TiE microscope with an A1R confocal system equipped with NIS-Elements 5.3 software. Z-stacks with steps 5 µm apart were taken using the 20x objective and final images shown in figures are max projections of the z-stack images.

Results

(1) Crithidia bombi *is sensitive to selecting compounds*

Genetic modification requires selection for cells that have taken up exogenous recombinant DNA molecules. In particular, the expression of fluorescent proteins facilitates detailed morphological analysis of parasites both *in vitro* and *in vivo*. Therefore, we sought to establish a protocol whereby plasmids driving expression of fluorescent proteins could be introduced into *C. bombi*. To do this, we first needed to determine sensitivity to antibiotics for which resistance genes

could be used as selectable markers. We monitored growth of *C. bombi* strain 08.076 [22] in 0, 5, 10, 20, 40 or 80 μg/ml of either hygromycin (Hyg) or neomycin (Neo, G418) over the course of four days (Fig 1). We found that *C. bombi* were sensitive to both drugs, with 40 μg/mL being the lowest concentration that completely inhibited growth after 20 hours.

(2) *Expression of cytoplasmic fluorescent proteins*

Next, we investigated methods for genetic modification of *C. bombi*. Some trypanosomatids can maintain circular plasmids as episomes [37–41]. This approach is advantageous in that it does not require stable integration by homologous recombination at a genomic locus. Using episomes simplifies construct creation, does not require detailed knowledge of the genome sequence, and can increase transfection efficiency. For this reason, we chose a series of plasmids originally developed for the congener *C. fasciculata*, a monoxenous parasite of mosquitoes, and *Leishmania*, a dixenous parasite of sand flies and mammals [24]. The pNUS-eGFP-cH plasmid (Fig 2a) contains genes for eGFP and Hyg resistance flanked by 5' and 3' untranslated regions (UTRs) derived from *C. fasciculata* [24]. UTRs direct processing of the mature transcript required for expression [42]. Similarly, pNUS-RFP-cN contains a gene encoding RFP and the Neo resistance gene (Fig 2a). We prepared each of these plasmids by ethanol precipitation and introduced them into the cultured *C. bombi* strain 08.076 by nucleofection using a protocol previously established for *C. fasciculata* [25]. After transfection, cells were returned to media in either 24-well plates or in tissue culture flasks and were left to recover for approximately 24 hours before addition of 40 μg/mL of either Hyg or Neo. For each transfection, a sample containing the same number of untransfected cells was placed under selection to confirm drug efficacy. After 10-12 days of selection, plates containing transfected cells had healthy, dividing cells, while no wells in the mock plates contained growing cells. Screening of transfected cells by fluorescence microscopy revealed eGFP or RFP expression, indicating successful transfection of the episomal pNUS-eGFP-cH plasmid (Fig 2b) and pNUS-RFP-cN plasmid (Fig 2c). In a separate experiment to estimate plating efficiency, we diluted parental 08.076 cells in media and plated serial dilutions in 96-well plates. After two weeks of growth, 78% of the expected wells had densely growing cells, so we estimate a plating efficiency of around 80%. Since every well in our transfection plates recovered, it is impossible to know whether individual wells were seeded with one or more transfected cells, but probably the cell lines obtained are not clonal. Selection in flasks, rather than plates, also resulted in recovered transfected cells within 10-12 days. We did not detect any instances of spontaneous Hyg or Neo resistance, as no cells were recovered from the "mock" treatment vessels.

To estimate transfection efficiency for the 08.076 cell line, we repeated the above procedure with 5 μg of purified plasmid DNA and 3 x 10^7 total *C. bombi* cells. Following transfection, we performed a series of 10-fold dilutions and plated these dilutions in 24 well plates. The next day, we added selecting drug and then monitored plates for cell growth for 9-16 days. Parasites transfected with the pNUS-eGFP-cH plasmid recovered after 11 days of selection. Examination of two randomly selected wells confirmed green fluorescence. For this plasmid, under these conditions, we estimate a transfection efficiency of 5 x 10^{-3} based on the number of wells scored positively for cell growth as a fraction of the number of cells plated in each dilution. Transfection with pNUS-RFP-cN under the same conditions resulted in an estimated transfection efficiency of 8 x 10^{-4}. The cells took longer to recover, and plates were scored at 16 days of

selection. Again, a subset of surviving wells (n=5) screened for red fluorescence were all positive.

We used the same procedure to introduce pNUS-GFP-cH into a different *C. bombi* isolate, 16.075 [43] (Fig 2b). As with 08.076, green fluorescence in transfected 16.075 cells was significantly above background (autofluorescence detectable in both isolates imaged with long exposures, Fig S1). Thus, our nucleofection procedure seems generalizable to more than one strain/isolate of culture-adapted *C. bombi.*

One disadvantage of modification by episomal plasmids is heterogeneity of expression, since each parasite can contain a different number of episomes that are imperfectly segregated during cell division [24,37]. Therefore, after several passages, we increased the concentration of Hyg or Neo from 40 μg/mL to 80 μg/mL to select for cells with higher episomal copy number, although expression levels still varied somewhat between cells. To confirm that eGFP- or RFP-expressing cells were fully drug resistant, we performed growth curves and found that, in contrast to parental strains, 08.076 *C. bombi* transfected with pNUS-eGFP-cH or pNUS-RFP-cN showed robust growth in the presence of 80 μg/mL of the appropriate selecting drug (Fig 2d, e).

(3) *Expression of fluorescent proteins with distinct subcellular localizations*

Crithidia bombi, like other trypanosomatids, are complex eukaryotic cells with a variety of compartments and a distinctly polarized subcellular organization [44,45]. In related species, subcellular organization can change as the parasite undergoes morphological and metabolic adaptation to different environments [45–48]. In addition to changes in cell and organelle shape, the localization of individual proteins can also vary during the cell and life cycle [45,49]. Determining the location of a particular protein can provide important clues to its function. For these reasons, it is useful to have markers for various subcellular compartments to monitor these organelles and to compare to the localization of uncharacterized proteins. For example, the mitochondrion of trypanosomatids is typically an elaborate branched network that extends throughout the cell. The dixenous trypanosomatid *Trypanosoma brucei* dramatically alters both mitochondrial shape and function as it alternates between mammalian and insect hosts [50]. The branched mitochondrial network can resemble other organelles, such as the endoplasmic reticulum, making colocalization with a known marker required to confirm the subcellular location of a protein [45]. Organelle-specific dyes, such as MitoTracker, can be useful for co-localization but they are dependent on membrane potential and dye toxicity, which can complicate imaging of live cells. Mitochondria are metabolic and signaling hubs whose function requires the post-translational import of hundreds of nuclear-encoded proteins. The function and proper localization of many of these proteins are likely required for survival and replication of *C. bombi* parasites.

To label the mitochondrion, we introduced a variation of pNUS-eGFP-cH in which a mitochondrial targeting signal from the related parasite *T. brucei* was fused to the open reading frame (ORF) of eGFP to produce pNUS-mitoeGFP-cH (Fig 3a) [25]. As observed in *C. fasciculata*, introducing this plasmid into *C. bombi* labels the branched tubular mitochondrion, which we verified by co-localization with MitoTracker (Fig 3b, Pearson's coefficient 0.829).

While alterations in mitochondrial shape could indicate changes in parasite metabolism, fluorescent nuclei would provide a clear identification of dividing cells. Determining the frequency of dividing cells in different insect tissues and at different stages of the infection would inform models for rates of colonization and infectivity of the insect host. To label the nucleus, we created a plasmid in which the ORF for the RNase H1 gene from *C. fasciculata* (*Cf*RNH1) was fused to eGFP at its C-terminus in pNUS-eGFP-cH to create pNUS-*Cf*RNH1eGFP-cH (Fig 3c). Introduction of this plasmid into *C. bombi* followed by Hyg selection resulted in cell lines expressing GFP in the nucleus as evidenced by co-localization with the DNA stain 4',6-diamidino-2-phenylindole, (DAPI) (Fig 3d). In *C. fasciculata*, earlier work showed that the gene for *Cf*RNH1 contains alternate start codons allowing for two versions of the protein, one of which contains a mitochondrial targeting signal [51]. In *C. bombi*, the *Cf*RNH1eGFP signal is concentrated in the nucleus, indicating that the dual localization of this enzyme may not occur. However, our construct included only the ORF (including both possible start codons) of *Cf*RNH1 but not the native 5' processing signal, which may be important for stability of the longer transcript [51]. DAPI stains both the nucleus and kinetoplast. The Pearson's coefficient for co-localization of *Cf*RNH1eGFP with DAPI was 0.392 reflecting overlap of nuclear signal only.

In order to colonize their insect host, *C. bombi* cells must attach via their flagella to the lining of the hindgut [5]. This allows the parasites to replicate as attached cells without being eliminated by defecation. In *C. fasciculata* and other species, this distinct developmental stage can also occur *in vitro* through contact with tissue culture plastic [23,48,52–56]. To see if this was the case for *C. bombi*, we allowed log-phase parasites to adhere to a plastic dish for 24 hours, followed by washing with 1X PBS to remove non-adherent cells. As in *C. fasciculata*, some cells attached and divided, producing attached groups of cells called rosettes. These rosettes could be imaged by live-cell fluorescent microscopy, allowing for visualization of fluorescent markers in both swimming and attached parasites (Fig 3e).

(4) *Visualizing parasites in* Bombus impatiens

While genetic modification of *C. bombi* will enable morphological and functional studies *in vitro*, it also has the potential to improve visualization of host-parasite interactions and the progress of infections in the natural host under different conditions. Both 08.076 and 16.075 parasite strains were isolated from *B. impatiens* and were culture adapted for sequence analysis and other studies [22,43]. However, mixed infections containing multiple distinct strains of *C. bombi* are common, and some variability between isolates might be expected [22,57]. In addition, extended passaging in culture could fundamentally change the biology of the organism. Therefore, we sought to modify a clonal isolate of *C. bombi* that had been recently obtained from a laboratory colony of *B. impatiens*. We dissected guts from infected bees, homogenized the tissue, transferred parasites to medium, and obtained clones by limiting dilution in 96-well plates in the presence of antibiotics and antifungals.

We selected one of these clones, WHA1, for further analysis. Since *C. bombi* and *C. expoeki* are distinct species with a high degree of morphological and genome conservation, we isolated DNA from WHA1 as well as our cultured 08.076 line to confirm species identity. Using the primers described in [32], we PCR amplified three gene targets: glycosomal glyceraldehyde phosphate dehydrogenase (*gGAPDH*), small subunit ribosomal RNA (*SSU rRNA*), and cytochrome B (*Cyt*

B). We purified these PCR products and performed Sanger sequencing. We then aligned the resulting reads to the reference *C. bombi* and *C. expoeki* sequences in GenBank (Fig S2). For the *Cyt B* region, we also amplified and sequenced DNA from the 08.076 *C. bombi* strain. Across the three target genes, there are 76 positions where the nucleotide sequence differs between *C. bombi* and *C. expoeki*. In 75 of these instances, the WHA1 sequence has the same nucleotide as the *C. bombi* sequence. Therefore, we conclude that the WHA1 isolate is *C. bombi*, and we will refer to it as *Cb*-WHA1. At one position, in the SSU rRNA gene, the WHA1 sequence was missing a nucleotide found in both the *C. bombi* and *C. expoeki* sequences, probably indicative of minor, within-species genetic variation.

We next used nucleofection to separately introduce the pNUS-eGFP-cH and pNUS-RFP-cN plasmids into WHA1 as described above. Following selection of drug-resistant lines, we confirmed fluorescence of cells cultured *in vitro* by microscopy. We then used these parasites (*Cb*-WHA1-GFP and *Cb*-WHA1-RFP) to infect commercial *B. impatiens* (Fig 4) and visualized fluorescent cells *in vivo*. As a negative control, microscopy was also completed on digestive tracts of uninfected *B. impatiens.* While there is some autofluorescence of the bumble bee tissue (Fig S3), particularly in the green channel, fluorescent parasites were clearly seen in the guts of the infected bees, attached as clusters to the lining of the hindgut and rectum.

Since antibiotic selection for episomal plasmids could not be maintained during infections *in vivo*, we tested the stability of the plasmid in the absence of selection in cultured cells. *Cb*-WHA1-RFP cells were passaged into media with or without 80 µg/ml neomycin (three identical flasks per treatment). Over a period of 22 days, we monitored fluorescence intensity by imaging live cells from each flask every 2-3 days and scoring cells with signal above or below a set threshold. Removal of neomycin was associated with a minor decrease in the number of cells above the fluorescence threshold (62% fluorescent in the presence of neomycin versus 53% fluorescent in the absence of neomycin, $\chi2= 3.8839$, $p = 0.048$). However, the number of days in each treatment ($\chi2= 0.4649$, $p = 0.495$) and the day by neomycin treatment interaction ($\chi2= 0.1524$, $p = 0.696$) did not affect variation in fluorescence. Thus, while expression of RFP was lower overall in the absence compared to presence of neomycin, expression did not decrease over a period of 22 days in either treatment, indicating stability over time (Fig S4).

Discussion

We present a method for introducing plasmids into *C. bombi* and selecting modified parasites with two different selectable markers. We have shown that 5' and 3' UTRs containing transcript-processing signals derived from *C. fasciculata* function for stable expression in *C. bombi*. In addition, introduction of transgenes bearing localization signals from other trypanosomatids direct similar subcellular localization patterns in *C. bombi*. These modifications improve visualization of cellular morphology of swimming and attached developmental forms, both of which can be generated *in vitro* under standard culture conditions. Genetically modified parasites also retained the ability to infect *B. impatiens*, facilitating detailed studies of host-pathogen interactions.

We successfully modified three independent isolates of *C. bombi*, one of which was isolated directly from a laboratory colony of *B. impatiens* as part of this study. Since the method appears to be both robust and generalizable, it might also be applied to the modification of other

pollinator pathogens, such as *Lotmaria passim*. The introduction of plasmids as episomes means that genome sequence data is not required, transfection efficiencies are relatively high, and the same series of plasmids may be used for different species and strains.

The transfection efficiency of *C. bombi*, which we estimate to be between 10^{-4} and 10^{-3} depending on the selection marker used, is higher than what we have measured for *C. fasciculata* under similar conditions (10^{-6}-10^{-5}, M.L. Povelones, unpublished results), and is comparable to or higher than what has been reported for other trypanosomatids, including procyclic (10^{-5}) and bloodstream (10^{-4}) form *T. brucei* [58] and *Leishmania* (10^{-3}) [59].

We observed that RFP-expressing *C. bombi* displayed much brighter fluorescence than eGFP-expressing cells, allowing for greater sensitivity *in vivo*. This could be due to variation in the amount of correlation between resistance to a particular drug and the average episomal copy number per cell of the selectable marker. Neomycin may select for parasites with larger numbers of episomes per cell, leading to a greater proportion of cells above the threshold for detection. The GFP construct, in contrast, was selected using hygromycin, which may require only a few copies of the resistance gene per cell to allow for growth. The difference in measured transfection efficiencies between Hyg and Neo-containing plasmids also supports this conclusion.

While we have focused on the production of fluorescent parasites to improve sensitivity and resolution for describing infection dynamics *in vivo*, we believe that there are many exciting applications of molecular genetic approaches in these parasites. For example, genome-wide gene expression data obtained through RNA sequencing has revealed transcripts that may enable parasite survival in the host [14]. Labeling these genes with epitope or fluorescent tags would enable researchers to follow their dynamic localization during infection and colonization of the gut. Such tagged proteins could also be used to purify protein complexes that allow parasite adaptation to host microenvironments or that function at the host-parasite interface. In strains for which a genome sequence is available, plasmid constructs could be created to modify genomic loci. This would allow for tagging a gene at its endogenous locus or, compellingly, creating stable genomic knockouts to evaluate gene function in parasite growth and host interactions.

Future research focused on the development of a reliable and quantitative attachment assay for parasites *in vitro* will allow investigators to examine the effects of culture conditions, including floral products, on growth and the developmental switch between swimming and attached forms, a transition that is likely critical for effective colonization of the bee gut. This attachment assay will permit rapid and mechanistic testing of hypotheses that can then be extended to the laboratory infection model and the interpretation of findings in field conditions. We believe that the introduction of molecular genetic tools for manipulation of *C. bombi* will enable integrative approaches across disciplines and scales to begin to bridge the knowledge gaps for how parasites impact bee pollinator health.

Figure Legends

Fig. 1 Cultured *Crithidia bombi* cells are sensitive to selecting drugs. Growth curves of *C. bombi* parental strain 08.076 [22] grown in FP-FB medium with increasing levels of **a)** hygromycin

(Hyg) or **b)** neomycin (Neo) to determine optimal concentration for selection. Each graph shows the mean of three independent replicates. Error bars are standard error.

Fig. 2 Genetic modification of *C. bombi* cells. **a)** Plasmid map of pNUS-eGFP-cH [24]. The open reading frames for enhanced green fluorescence protein (eGFP), hygromycin resistance (HygR) and ampicillin resistance (ampR, for propagation of plasmids in *E. coli*), as well as 5' and 3' UTRs from the phosphoglycerate kinase (PGK) and glutathione synthetase (GSS) genes including sequences for transcript processing are shown. Plasmid map of pNUS-RFP-cN [24] showing open reading frames encoding red fluorescence protein (RFP), neomycin resistance (NeoR), and ampR as well as 5' and 3' UTRs. **b)** *C. bombi* strains 08.076 [22] and 16.075 [33] nucleofected with the pNUS-eGFP-cH plasmid. BF, brightfield (visible light); eGFP, enhanced green fluorescent protein signal visible in the green channel; DAPI, DNA stain. Mitochondrial DNA (kinetoplast, K) and the nucleus (N) in a single cell are indicated with arrowheads. Fluorescent images are z-stack maximum projections. Scale bar is 5 µm. **c)** *C. bombi* strain 08.076 harboring the pNUS-RFP-cN plasmid imaged in brightfield (BF), red fluorescence channel (RFP), and with DAPI. K, kinetoplast DNA; N, nucleus. Scale bar is 5 µm. **d)** Growth curve of *C. bombi* strain 08.076 bearing the pNUS-eGFP-cH plasmid in 0 or 80 µg/mL Hyg. For each condition, the mean of three replicates is shown. Error bars are standard error. **e)** Growth curve of *C. bombi* strain 08.076 bearing the pNUS-RFP-cN plasmid in 0 or 80 µg/mL Neo. For each condition, the mean of three replicates is shown. Error bars are standard error.

Fig. 3 Organelle markers for mitochondria and nuclei in *C. bombi*. **a)** Plasmid map of a construct for episomal expression of a mitochondrion-targeted eGFP [25]. 5' and 3' UTRs for transcript processing and stability are shown in gray. PGK, phosphoglycerate kinase; GSS, glutathione synthetase; MTS, mitochondria targeting signal; eGFP, enhanced GFP; HygR, hygromycin resistance; ampR, ampicillin resistance. Some relevant restriction enzyme sites are also shown. **b)** *C. bombi* strain 16.075 [33] nucleofected with pNUS-mitoGFP-cH. BF, brightfield; eGFP, mitochondrial eGFP fluorescence; MitoTracker, membrane potential dependent mitochondrial red fluorescent dye; DAPI, DNA stain (N, nucleus; K, kinetoplast). Merge shows overlay of fluorescent channels. Scale bar is 5 µm. **c)** Plasmid map of pNUS-*Cf*RNH1eGFP-cH. *Cf*RNH1, RNH1 gene from *Crithidia fasciculata*. Other abbreviations as in (a). Some relevant restriction enzyme sites are shown. **d)** Swimming *C. bombi* strain 08.076 [22] nucleofected with the pNUS-*Cf*RNH1eGFP-cH plasmid showing nuclear expression of eGFP-tagged *Cf*RNH1 (eGFP); DAPI, DNA stain (N, nucleus; K, kinetoplast); brightfield (BF); and merge of fluorescent channels. Scale bar is 5 µm. **e)** 08.076 *C. bombi* cells growing as attached rosettes on a MatTek dish and expressing pNUS-*Cf*RNH1eGFP-cH were imaged live in brightfield (BF) and in the green channel to show nuclear localization of *Cf*RNH1eGFP. Scale bar is 5 µm.

Fig. 4 Visualizing fluorescent parasites *in vivo*. **a)** The ileum of bees infected with parasites expressing pNUS-eGFP-cH (panels 2-4) were compared to the ileum of uninfected bees (panel 1). Arrowhead indicates a cluster of eGFP-positive parasites (panel 2). The dotted box in panel 3 shows the area of enlargement in panel 4. Panel 4 shows fluorescence in the green channel only. Panels 1-3 are merges of red and green fluorescence plus brightfield. Scale bars are as shown. **b)** The ileum of an uninfected bee (panel 1) compared to sections of the ileum from bees infected with *C. bombi* parasites expressing pNUS-RFP-cN (panels 2-4). The dotted box in panel 3 shows

the area of enlargement in panel 4. All images are z-stack max projections and merges of red fluorescence, green fluorescence, and brightfield. Scale bars are as shown.

Fig. S1 *Crithidia bombi* parental strains do not show fluorescence. **a)** Parental strain *C. bombi* 08.076 imaged for brightfield (BF), green fluorescence (eGFP) and DAPI. K, kinetoplast; N, nucleus. **b)** Parental strain *C. bombi* 08.076 images for brightfield, red fluorescence, and DAPI. **c)** Parental strain *C. bombi* 16.075 imaged for brightfield, green fluorescence, and DAPI. All images are z-stack maximum projections. Scale bar is 5 μm.

Fig. S2 Confirmation that *Cb*-WHA1 is a *Crithidia bombi* strain. **a)** *gGAPDH* amplified from *Cb*-WHA1 and sequenced using primers described in [32] is shown aligned with the same region from *C. bombi* (Cb, GenBank accession number GU321192) and *C. expoeki* (Ce, GenBank accession number GU321193). **b)** A region of the *SSU rRNA* gene amplified from *Cb*-WHA1 and sequenced is aligned to the corresponding regions of *C. bombi* (Cb, GenBank accession number GU321194) and *C. expoeki* (Ce, GenBank accession number GU321195). **c)** Cyt B was amplified and sequenced from cultured CbWHA1 and 08.076 strains and compared to the same region in two strains of *C. bombi* (GenBank accession numbers GU3211187 and GU321188) and two strains of *C. expoeki* (GenBank accession numbers GU321189 and GU321190).

Fig. S3 *Crithidia bombi* expressing fluorescent transgenes can be imaged *in vivo*. The ileum of uninfected *B. impatiens* **(A-C)** and *B. impatiens* infected with either GFP **(D-G)** or RFP **(H-K)** - expressing *C. bombi* were imaged by confocal microscopy for green fluorescence (GFP), red fluorescence (RFP) and brightfield (TD). In G clusters of parasites are indicated by arrows. Some autofluorescence is detectable in both green and red channels that is distinguishable from fluorescent parasites. Scale bars are as shown.

Fig. S4 Episomal fluorescence is stable in the absence of selection. Triplicate flasks were grown in the absence (orange) or presence (green) of neomycin selection for 22 days. Every 2-3 days, a sample was removed and cells scored for red fluorescence using live cell fluorescence microscopy. Values show the number of cells with red fluorescence as a proportion of total cells as a function of the number of days cultured. Cells were passaged as usual in the appropriate media (without or with neomycin).

References

1. Lukeš J, Skalický T, Týč J, Votýpka J, Yurchenko V. Evolution of parasitism in kinetoplastid flagellates. Molecular and Biochemical Parasitology. 2014;195: 115–122. doi:10.1016/j.molbiopara.2014.05.007

2. Horn D. A profile of research on the parasitic trypanosomatids and the diseases they cause. Buscaglia CA, editor. PLoS Negl Trop Dis. 2022;16: e0010040. doi:10.1371/journal.pntd.0010040

3. Maslov DA, Votýpka J, Yurchenko V, Lukeš J. Diversity and phylogeny of insect trypanosomatids: all that is hidden shall be revealed. Trends in Parasitology. 2012;29: 43–52. doi:10.1016/j.pt.2012.11.001

4. Frolov AO, Kostygov AY, Yurchenko V. Development of Monoxenous Trypanosomatids and Phytomonads in Insects. Trends in Parasitology. 2021;37: 538–551. doi:10.1016/j.pt.2021.02.004

5. Vickerman K, Tetley L. Flagellar Surfaces of Parasitic Protozoa and Their Role in Attachment. In: Bloodgood RA, editor. Ciliary and Flagellar Membranes. Boston, MA: Springer US; 1990. pp. 267–304. doi:10.1007/978-1-4613-0515-6_11

6. Povelones ML, Holmes NA, Povelones M. A sticky situation: When trypanosomatids attach to insect tissues. PLOS Pathogens. 2023;19: e1011854. doi:10.1371/journal.ppat.1011854

7. Goulson D, Nicholls E, Botías C, Rotheray EL. Bee declines driven by combined stress from parasites, pesticides, and lack of flowers. Science. 2015;347: 1255957. doi:10.1126/science.1255957

8. Ngor L, Palmer-Young EC, Nevarez RB, Russell KA, Leger L, Giacomini SJ, et al. Cross-infectivity of honey and bumble bee-associated parasites across three bee families. Parasitology. 2020;147: 1290–1304. doi:10.1017/S0031182020001018

9. Gegear RJ, Otterstatter MC, Thomson JD. Bumble-bee foragers infected by a gut parasite have an impaired ability to utilize floral information. Proceedings of the Royal Society B: Biological Sciences. 2006;273: 1073–1078. doi:10.1098/rspb.2005.3423

10. Brown MJF, Schmid-Hempel R, Schmid-Hempel P. Strong context-dependent virulence in a host–parasite system: reconciling genetic evidence with theory. Journal of Animal Ecology. 2003;72: 994–1002. doi:10.1046/j.1365-2656.2003.00770.x

11. Brown MJF, Loosli R, Schmid-Hempel P. Condition-dependent expression of virulence in a trypanosome infecting bumblebees. Oikos. 2000;91: 421–427. doi:10.1034/j.1600-0706.2000.910302.x

12. Gómez-Moracho T, Buendía-Abad M, Benito M, García-Palencia P, Barrios L, Bartolomé C, et al. Experimental evidence of harmful effects of *Crithidia mellificae* and *Lotmaria passim* on honey bees. International Journal for Parasitology. 2020;50: 1117–1124. doi:10.1016/j.ijpara.2020.06.009

13. Deshwal S, Mallon EB. Antimicrobial peptides play a functional role in bumblebee anti-trypanosome defense. Dev Comp Immunol. 2014;42: 240–243. doi:10.1016/j.dci.2013.09.004

14. Liu Q, Lei J, Darby AC, Kadowaki T. Trypanosomatid parasite dynamically changes the transcriptome during infection and modifies honey bee physiology. Commun Biol. 2020;3: 1–8. doi:10.1038/s42003-020-0775-x

15. Koch H, Woodward J, Langat MK, Brown MJF, Stevenson PC. Flagellum removal by a nectar metabolite inhibits infectivity of a bumblebee parasite. Current Biology. 2019;29: 3494-3500.e5. doi:10.1016/j.cub.2019.08.037

16. Figueroa LL, Fowler A, Lopez S, Amaral VE, Koch H, Stevenson PC, et al. Sunflower spines and beyond: Mechanisms and breadth of pollen that reduce gut pathogen infection in the common eastern bumble bee. Functional Ecology. n/a. doi:10.1111/1365-2435.14320

17. Fowler AE, Stone EC, Irwin RE, Adler LS. Sunflower pollen reduces a gut pathogen in worker and queen but not male bumble bees. Ecological Entomology. 2020;45: 1318–1326. doi:10.1111/een.12915

18. Giacomini JJ, Leslie J, Tarpy DR, Palmer-Young EC, Irwin RE, Adler LS. Medicinal value of sunflower pollen against bee pathogens. Sci Rep. 2018;8: 14394. doi:10.1038/s41598-018-32681-y

19. LoCascio GM, Aguirre L, Irwin RE, Adler LS. Pollen from multiple sunflower cultivars and species reduces a common bumblebee gut pathogen. Royal Society Open Science. 2019;6: 190279. doi:10.1098/rsos.190279

20. Malfi RL, McFrederick QS, Lozano G, Irwin RE, Adler LS. Sunflower plantings reduce a common gut pathogen and increase queen production in common eastern bumblebee colonies. Proceedings of the Royal Society B: Biological Sciences. 2023;290: 20230055. doi:10.1098/rspb.2023.0055

21. Fowler AE, Giacomini JJ, Connon SJ, Irwin RE, Adler LS. Sunflower pollen reduces a gut pathogen in the model bee species, *Bombus impatiens*, but has weaker effects in three wild congeners. Proceedings of the Royal Society B: Biological Sciences. 2022;289: 20211909. doi:10.1098/rspb.2021.1909

22. Salathé R, Tognazzo M, Schmid-Hempel R, Schmid-Hempel P. Probing Mixed-Genotype Infections I: Extraction and Cloning of Infections from Hosts of the Trypanosomatid *Crithidia bombi*. Hughes W, editor. PLoS ONE. 2012;7: e49046. doi:10.1371/journal.pone.0049046

23. Filosa JN, Berry CT, Ruthel G, Beverley SM, Warren WC, Tomlinson C, et al. Dramatic changes in gene expression in different forms of *Crithidia fasciculata* reveal potential mechanisms for insect-specific adhesion in kinetoplastid parasites. Acosta-Serrano A, editor. PLoS Negl Trop Dis. 2019;13: e0007570. doi:10.1371/journal.pntd.0007570

24. Tetaud E, Lecuix I, Sheldrake T, Baltz T, Fairlamb AH. A new expression vector for *Crithidia fasciculata* and *Leishmania*. Molecular and Biochemical Parasitology. 2002;120: 195–204. doi:10.1016/S0166-6851(02)00002-6

25. DiMaio J, Ruthel G, Cannon JJ, Malfara MF, Povelones ML. The single mitochondrion of the kinetoplastid parasite *Crithidia fasciculata* is a dynamic network. López Lluch G, editor. PLoS ONE. 2018;13: e0202711. doi:10.1371/journal.pone.0202711

26. Burkard GS, Jutzi P, Roditi I. Genome-wide RNAi screens in bloodstream form trypanosomes identify drug transporters. Molecular & Biochemical Parasitology. 2011;175: 91–94. doi:10.1016/j.molbiopara.2010.09.002

27. Bolte S, Cordelières FP. A guided tour into subcellular colocalization analysis in light microscopy. Journal of Microscopy. 2006;224: 213–232. doi:10.1111/j.1365-2818.2006.01706.x

28. Schindelin J, Arganda-Carreras I, Frise E, Kaynig V, Longair M, Pietzsch T, et al. Fiji: an open-source platform for biological-image analysis. Nat Methods. 2012;9: 676–682. doi:10.1038/nmeth.2019

29. Brooks ME, Kristensen K, van Benthem KJ, Magnusson A, Berg CW, Nielsen A, et al. glmmTMB balances speed and flexibility among packages for zero-inflated generalized linear mixed modeling. The R journal. 2017;9: 378–400. doi:10.3929/ethz-b-000240890

30. Fox J, Weisberg S. An R Companion to Applied Regression. SAGE Publications; 2018.

31. Hartig F, Hartig M. Package 'DHARMa.' R Package Available online: https://CRAN R-project org/package= DHARMa (accessed on 5 September 2022). 2022.

32. Schmid-Hempel R, Tognazzo M. Molecular Divergence Defines Two Distinct Lineages of Crithidia bombi (Trypanosomatidae), Parasites of Bumblebees. Journal of Eukaryotic Microbiology. 2010;57: 337–345. doi:10.1111/j.1550-7408.2010.00480.x

33. Pérez-Morga D, Englund PT. The structure of replicating kinetoplast DNA networks. Journal of Cell Biology. 1993;123: 1069–1079. doi:10.1083/jcb.123.5.1069

34. Spurley WJ, Fisher KJ, Langdon QK, Buh KV, Jarzyna M, Haase MAB, et al. Substrate, temperature, and geographical patterns among nearly 2,000 natural yeast isolates. Yeast. 2022;39: 55–68. doi:10.1002/yea.3679

35. Madeira F, Pearce M, Tivey ARN, Basutkar P, Lee J, Edbali O, et al. Search and sequence analysis tools services from EMBL-EBI in 2022. Nucleic Acids Res. 2022;50: W276–W279. doi:10.1093/nar/gkac240

36. Waterhouse AM, Procter JB, Martin DMA, Clamp M, Barton GJ. Jalview Version 2—a multiple sequence alignment editor and analysis workbench. Bioinformatics. 2009;25: 1189–1191. doi:10.1093/bioinformatics/btp033

37. Roberts SC. The genetic toolbox for *Leishmania* parasites. Bioeng Bugs. 2011;2: 320–326. doi:10.4161/bbug.2.6.18205

38. Patnaik P k., Kulkarni S k., Cross G a. Autonomously replicating single-copy episomes in *Trypanosoma brucei* show unusual stability. The EMBO Journal. 1993;12: 2529–2538. doi:10.1002/j.1460-2075.1993.tb05908.x

39. Bellofatto V, Torres-Muñoz JE, Cross GA. Stable transformation of *Leptomonas seymouri* by circular extrachromosomal elements. Proc Natl Acad Sci U S A. 1991;88: 6711–6715.

40. Biebinger S, Clayton C. A Plasmid Shuttle Vector Bearing an rRNA Promoter Is Extrachromosomally Maintained in *Crithidia fasciculata*. Experimental Parasitology. 1996;83: 252–258. doi:10.1006/expr.1996.0072

41. Kelly JM, ward HM, Miles MA, Kendall G. A shuttle vector which facilitates the expression of transfected genes in *Trypanosoma cruzi* and *Leishmania*. Nucleic Acids Research. 1992;20: 3963–3969. doi:10.1093/nar/20.15.3963

42. Clayton C. Regulation of gene expression in trypanosomatids: living with polycistronic transcription. Open Biol. 2019;9: 190072. doi:10.1098/rsob.190072

43. Palmer-Young EC, Calhoun AC, Mirzayeva A, Sadd BM. Effects of the floral phytochemical eugenol on parasite evolution and bumble bee infection and preference. Sci Rep. 2018;8: 2074. doi:10.1038/s41598-018-20369-2

44. Gull K. The cytoskeleton of trypanosomatid parasites. Annual Review of Microbiology. 1999;53: 629–655. doi:10.1146/annurev.micro.53.1.629

45. Halliday C, Billington K, Wang Z, Madden R, Dean S, Sunter JD, et al. Cellular landmarks of *Trypanosoma brucei* and *Leishmania mexicana*. Mol Biochem Parasitol. 2019;230: 24–36. doi:10.1016/j.molbiopara.2018.12.003

46. Haanstra JR, González-Marcano EB, Gualdrón-López M, Michels PAM. Biogenesis, maintenance and dynamics of glycosomes in trypanosomatid parasites. Biochim Biophys Acta. 2016;1863: 1038–1048. doi:10.1016/j.bbamcr.2015.09.015

47. Wheeler RJ, Gluenz E, Gull K. The cell cycle of *Leishmania*: morphogenetic events and their implications for parasite biology. Molecular Microbiology. 2011;79: 647–662. doi:10.1111/j.1365-2958.2010.07479.x

48. Yanase R, Moreira-Leite F, Rea E, Wilburn L, Sádlová J, Vojtkova B, et al. Formation and three-dimensional architecture of *Leishmania* adhesion in the sand fly vector. Zamboni DS, Akhmanova A, editors. eLife. 2023;12: e84552. doi:10.7554/eLife.84552

49. Billington K, Halliday C, Madden R, Dyer P, Barker AR, Moreira-Leite FF, et al. Genome-wide subcellular protein map for the flagellate parasite *Trypanosoma brucei*. Nat Microbiol. 2023;8: 533–547. doi:10.1038/s41564-022-01295-6

50. Verner Z, Basu S, Benz C, Dixit S, Dobáková E, Faktorová D, et al. Malleable Mitochondrion of *Trypanosoma brucei*. Elsevier Ltd; 2015. doi:10.1016/bs.ircmb.2014.11.001

51. Engel ML. The *Crithidia fasciculata* RNH1 gene encodes both nuclear and mitochondrial isoforms of RNase H. Nucleic Acids Research. 2001;29: 725–731. doi:10.1093/nar/29.3.725

52. Maraghi S, Mohamed HA, Wallbanks KR, Molyneux DH. Scratched plastic as a substrate for trypanosomatid attachment. Annals of tropical medicine and parasitology. 1987;81: 457–458.

53. Hommel M, Robertson E. In vitro attachment of trypanosomes to plastic. Experientia. 1976;32: 464–466.

54. Skalický T, Dobáková E, Wheeler RJ, Tesařová M, Flegontov P, Jirsová D, et al. Extensive flagellar remodeling during the complex life cycle of *Paratrypanosoma*, an early-branching trypanosomatid. Proceedings of the National Academy of Sciences. 2017;114: 11757–11762. doi:10.1073/pnas.1712311114

55. Scolaro EJ, Ames RP, Brittingham A. Growth-Phase Dependent Substrate Adhesion in *Crithidia fasciculata*. Journal of Eukaryotic Microbiology. 2005;52: 17–22. doi:https://doi.org/10.1111/j.1550-7408.2005.3315r.x

56. Wakid MH, Bates PA. Flagellar attachment of *Leishmania* promastigotes to plastic film in vitro. Experimental Parasitology. 2004;106: 173–178. doi:10.1016/j.exppara.2004.03.001

57. Schmid-Hempel P, Reber Funk C. The distribution of genotypes of the trypanosome parasite, *Crithidia bombi*, in populations of its host, *Bombus terrestris*. Parasitology. 2004;129: 147–158. doi:10.1017/s0031182004005542

58. Burkard G, Fragoso CM, Roditi I. Highly efficient stable transformation of bloodstream forms of Trypanosoma brucei. Molecular & Biochemical Parasitology. 2007;153: 220–223. doi:10.1016/j.molbiopara.2007.02.008

59. Robinson KA, Beverley SM. Improvements in transfection efficiency and tests of RNA interference (RNAi) approaches in the protozoan parasite Leishmania. Molecular & Biochemical Parasitology. 2003;128: 217–228. doi:10.1016/s0166-6851(03)00079-3

Statements and Declarations

Funding This work was supported by a National Science Foundation IntBIO award number 2128223 to LSA and MLP. This work was also supported by a Lotta Crabtree Fellowship from the University of Massachusetts Amherst as well as the CAFE Hatch Award to SKG. This material is based upon work supported by the National Institute of Food and Agriculture, U.S. Department of Agriculture, and the Center for Agriculture, Food and the Environment at University of Massachusetts Amherst, under project number NE2001. The contents are solely the responsibility of the authors and do not necessarily represent the official views of the USDA or NIFA.

Competing Interests The authors declare no competing interests.

Author Contribution BVB, SGL, SKG, LSA, and MLP conceived of the ideas and designed experiments. BVB, SGL, SKG, FAS, and MLP implemented the experiments and collected the data. BVB, SGL, FAS, SKG, and MLP contributed to visualization. BVB, SGL, SKG, and MLP

wrote the first draft of the manuscript. All authors contributed critically to manuscript edits and gave final approval for publication.

Data Availability Data from this study have been made publicly available at the Dryad Digital Repository (doi:10.5061/dryad.hqbzkh1qt). Additional data, including plasmid sequences, are available upon request.

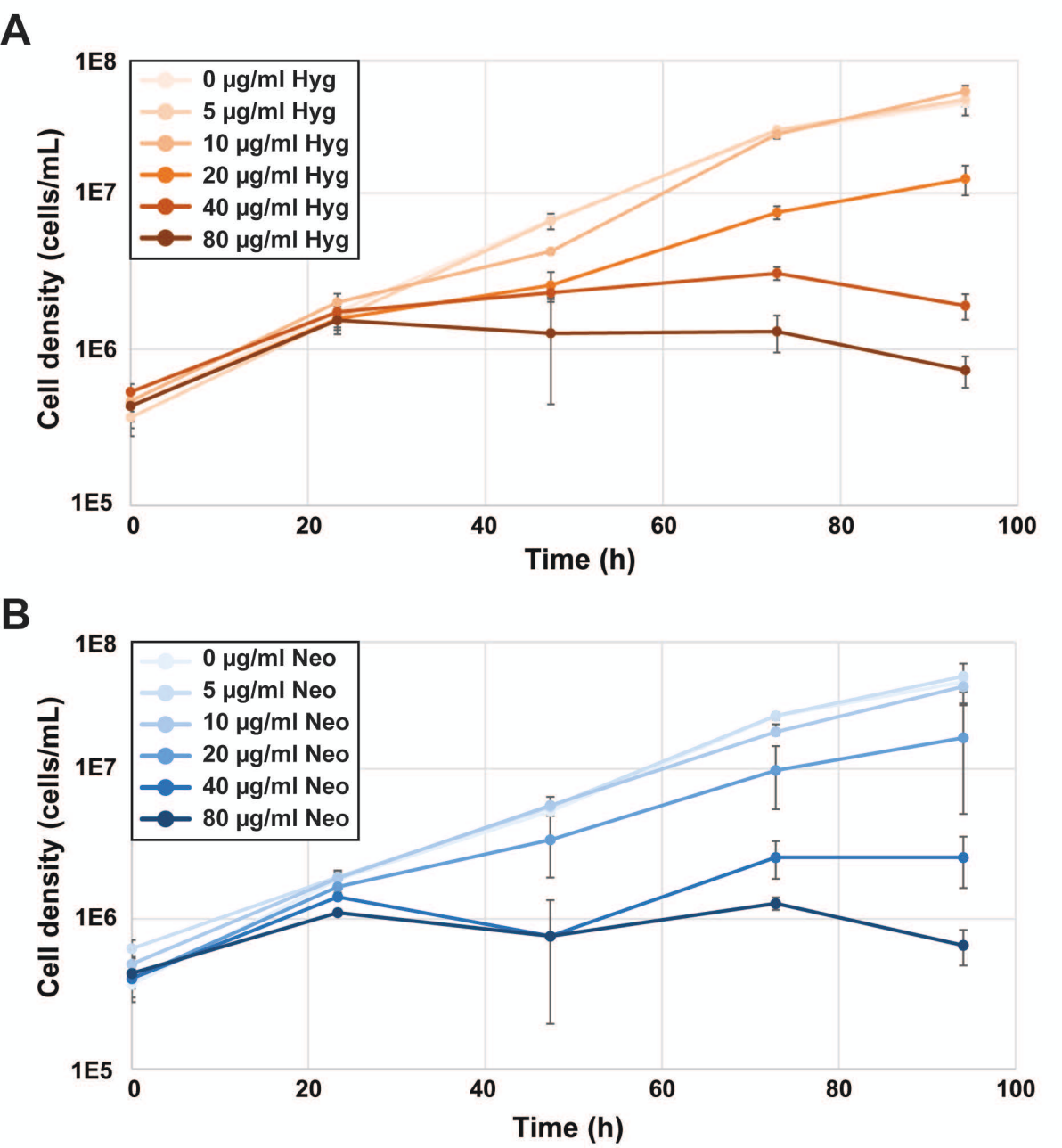
A
1E8
1E7
1E6
1E5
Cell density (cells/mL)
0 µg/ml Hyg
5 µg/ml Hyg
10 µg/ml Hyg
20 µg/ml Hyg
40 µg/ml Hyg
80 µg/ml Hyg
0
20
40
60
80
100
Time (h)
B
1E8
1E7
1E6
1E5
Cell density (cells/mL)
0 µg/ml Neo
5 µg/ml Neo
10 µg/ml Neo
20 µg/ml Neo
40 µg/ml Neo
80 µg/ml Neo
0
20
40
60
80
100
Time (h)

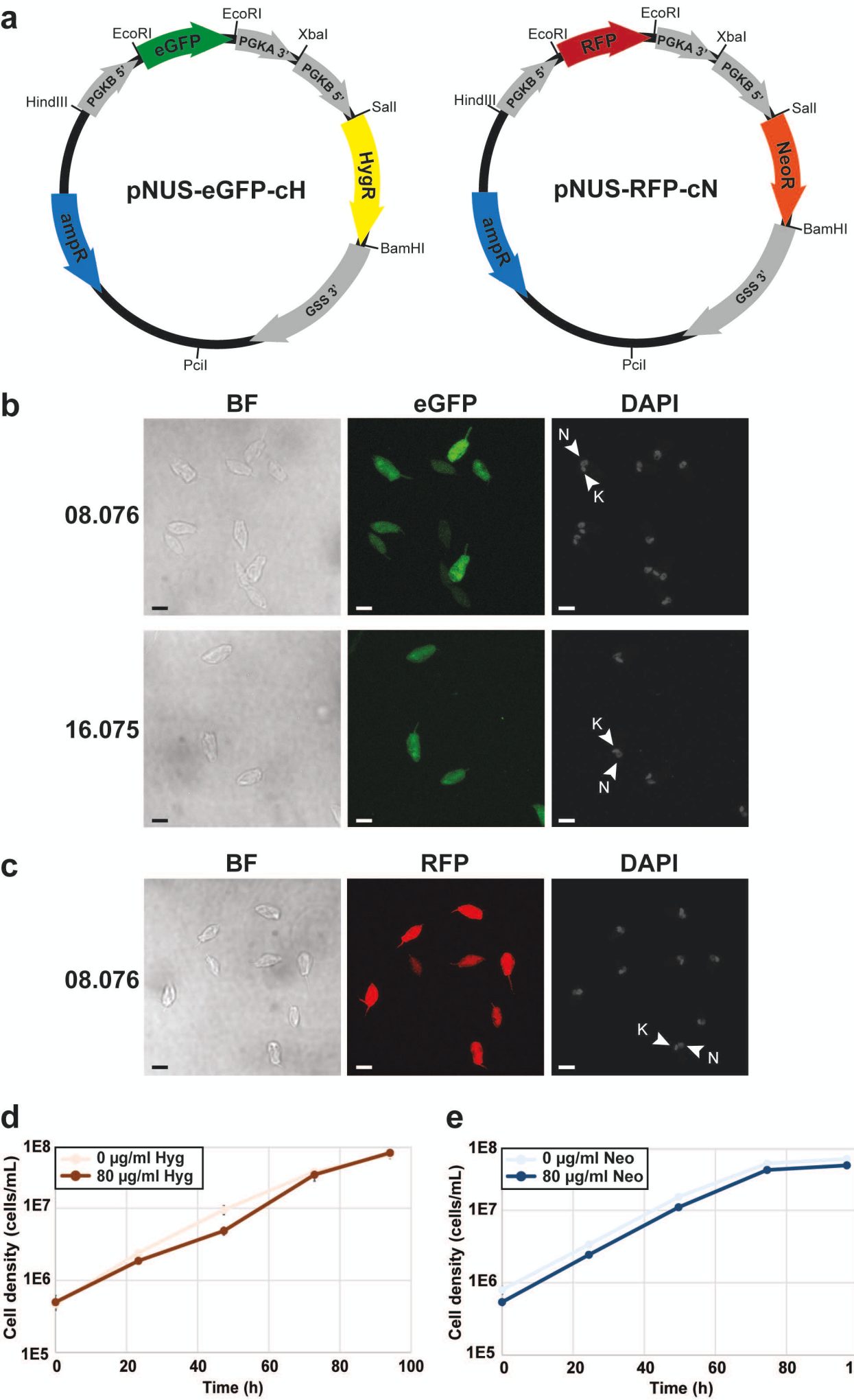
a
EcoRI
eGFP
EcoRI
PGKA 3'
XbaI
PGKB 5'
HindIII
PGKB 5'
SalI
HygR
pNUS-eGFP-cH
ampR
BamHI
GSS 3'
PciI
EcoRI
RFP
EcoRI
PGKA 3'
XbaI
PGKB 5'
HindIII
PGKB 5'
SalI
NeoR
pNUS-RFP-cN
ampR
BamHI
GSS 3'
PciI
b
BF
eGFP
DAPI
08.076
N
K
16.075
K
N
c
BF
RFP
DAPI
08.076
K
N
d
Cell density (cells/mL)
1E8
1E7
1E6
1E5
0 μg/ml Hyg
80 μg/ml Hyg
0
20
40
60
80
100
Time (h)
e
Cell density (cells/mL)
1E8
1E7
1E6
1E5
0 μg/ml Neo
80 μg/ml Neo
0
20
40
60
80
100
Time (h)

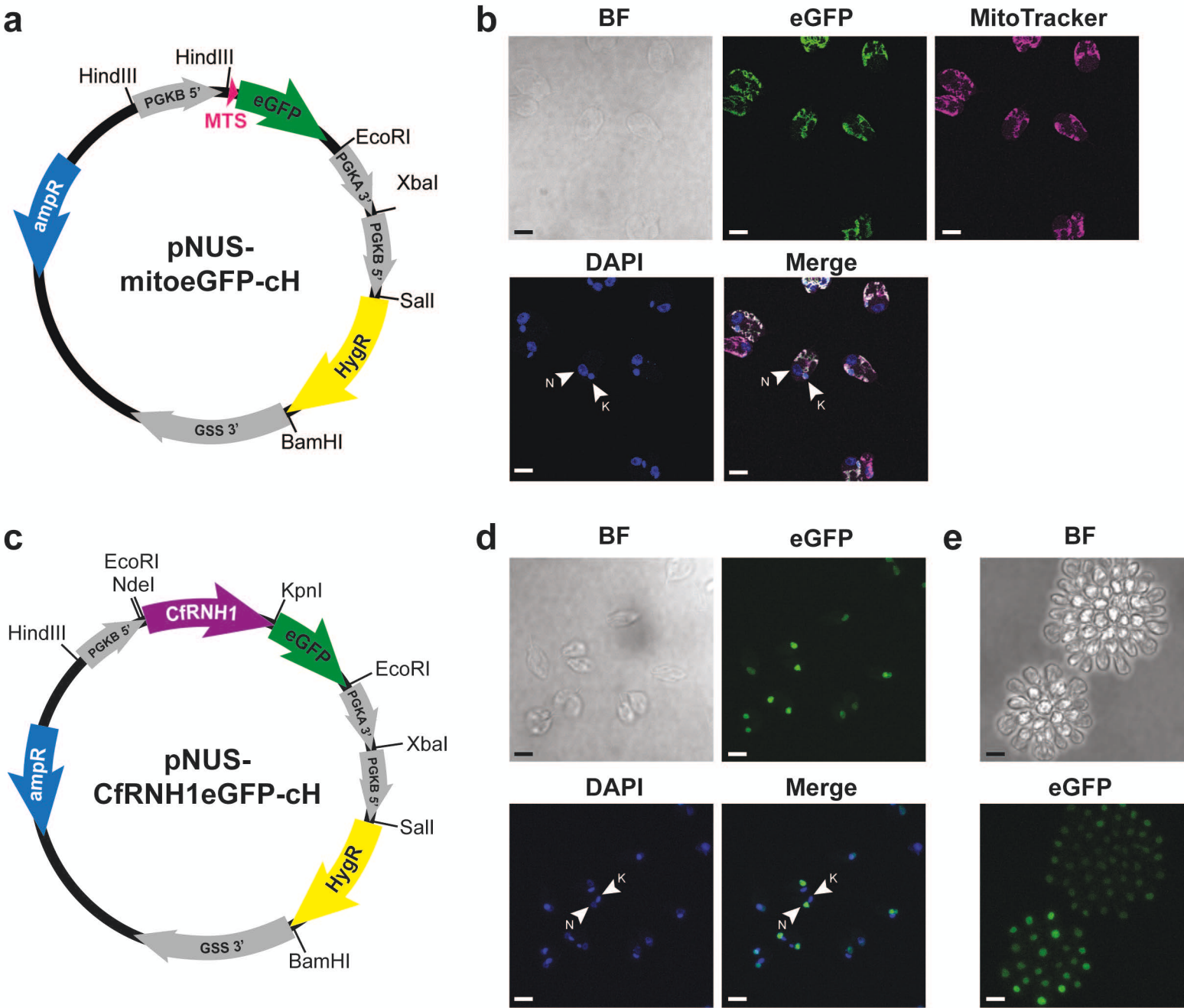
a
HindIII
HindIII
PGKB 5'
MTS
eGFP
EcoRI
PGKA 3'
XbaI
PGKB 5'
SalI
HygR
GSS 3'
BamHI
ampR
pNUS-
mitoeGFP-cH
b
BF
eGFP
MitoTracker
DAPI
Merge
N
K
c
EcoRI
NdeI
CfRNH1
KpnI
HindIII
PGKB 5'
eGFP
EcoRI
PGKA 3'
XbaI
PGKB 5'
SalI
HygR
GSS 3'
BamHI
ampR
pNUS-
CfRNH1eGFP-cH
d
BF
eGFP
DAPI
Merge
N
K
e
BF
eGFP

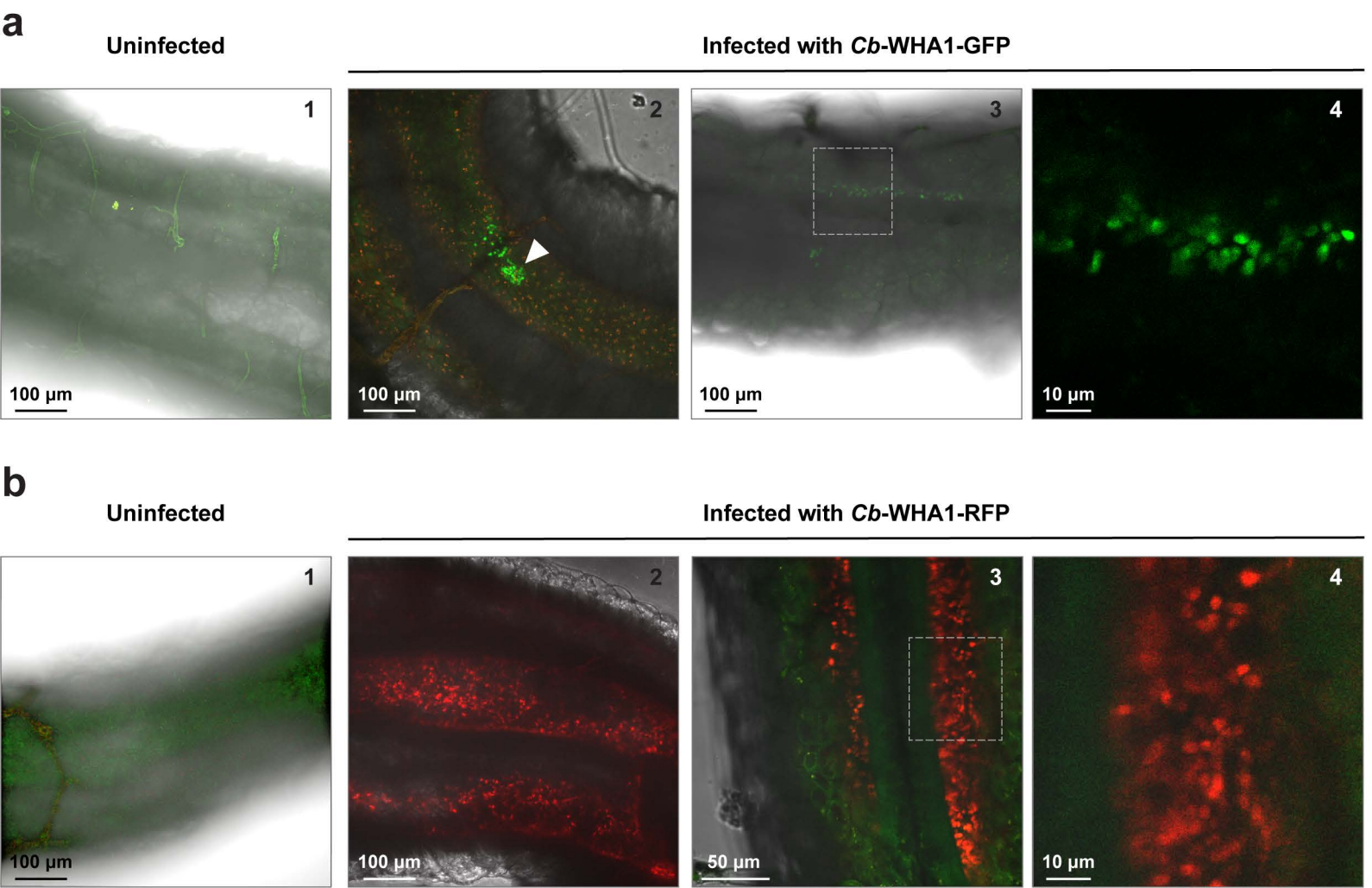
a
Uninfected
Infected with Cb-WHA1-GFP
1
2
3
4
100 µm
100 µm
100 µm
10 µm
b
Uninfected
Infected with Cb-WHA1-RFP
1
2
3
4
100 µm
100 µm
50 µm
10 µm

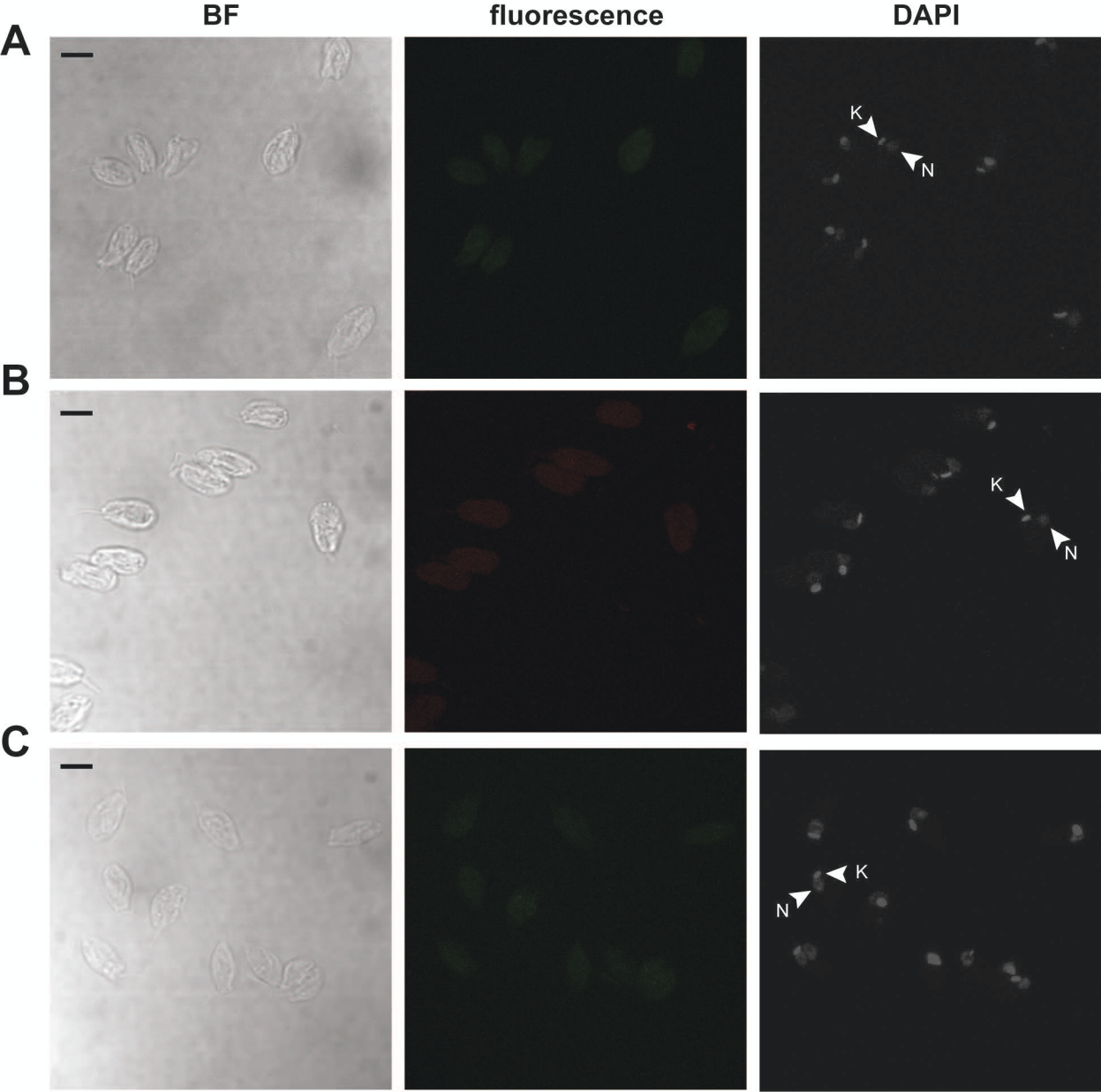
BF
fluorescence
DAPI
A
B
C
K
N
K
N
K
N

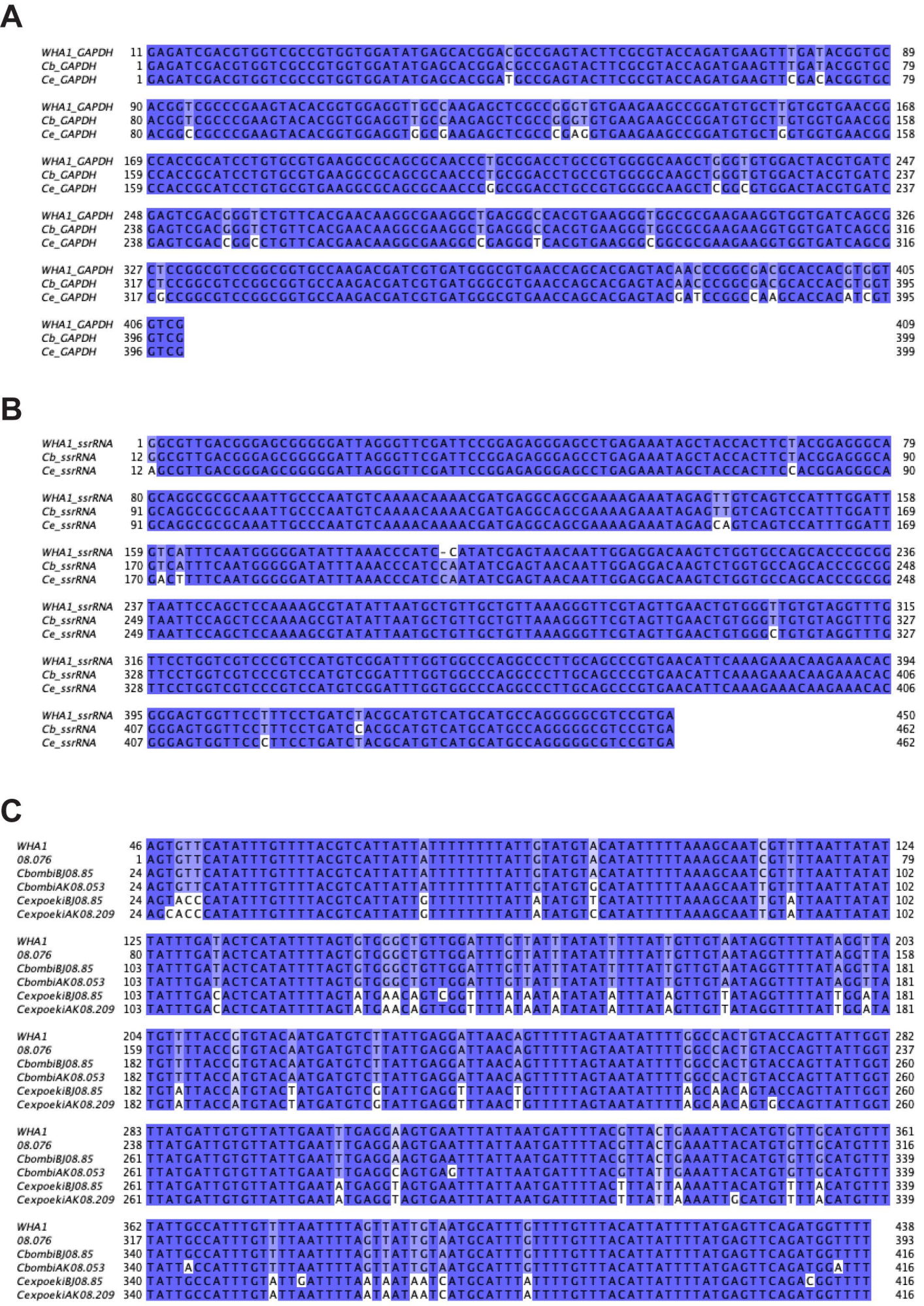
A
WHA1_GAPDH 11 GAGATCGACGTGGTCGCCGTGGTGGATATGAGCACGGACGCCGAGTACTTCGCGTACCAGATGAAGTTTGATACGGTGC 89
Cb_GAPDH 1 GAGATCGACGTGGTCGCCGTGGTGGATATGAGCACGGACGCCGAGTACTTCGCGTACCAGATGAAGTTTGATACGGTGC 79
Ce_GAPDH 1 GAGATCGACGTGGTCGCCGTGGTGGATATGAGCACGGATGCCGAGTACTTCGCGTACCAGATGAAGTTCGACACGGTGC 79
WHA1_GAPDH 90 ACGGTCGCCCCGAAGTACACGGTGGAGGTTGCCAAGAGCTCGCCGGGTGTGAAGAAGCCGGATGTGCTTGTGGTGAACGG 168
Cb_GAPDH 80 ACGGTCGCCCCGAAGTACACGGTGGAGGTTGCCAAGAGCTCGCCGGGTGTGAAGAAGCCGGATGTGCTTGTGGTGAACGG 158
Ce_GAPDH 80 ACGGCCGCCCCGAAGTACACGGTGGAGGTGGCGAAGAGCTCGCCCGAGGTGAAGAAGCCGGATGTGCTGGTGGTGAACGG 158
WHA1_GAPDH 169 CCACCGCATCCTGTGCGTGAAGGCGCAGCGCAACCCTGCGGACCTGCCGTGGGGCAAGCTGGGTGTGGACTACGTGATC 247
Cb_GAPDH 159 CCACCGCATCCTGTGCGTGAAGGCGCAGCGCAACCCTGCGGACCTGCCGTGGGGCAAGCTGGGTGTGGACTACGTGATC 237
Ce_GAPDH 159 CCACCGCATCCTGTGCGTGAAGGCGCAGCGCAACCCGGCGGACCTGCCGTGGGGCAAGCTCGGCGTGGACTACGTGATC 237
WHA1_GAPDH 248 GAGTCGACGGGTCTGTTCACGAACAAGGCGAAGGCTGAGGGCCACGTGAAGGGTGGCGCGAAGAAGGTGGTGATCAGCG 326
Cb_GAPDH 238 GAGTCGACGGGTCTGTTCACGAACAAGGCGAAGGCTGAGGGCCACGTGAAGGGTGGCGCGAAGAAGGTGGTGATCAGCG 316
Ce_GAPDH 238 GAGTCGACCGGCCTGTTCACGAACAAGGCGAAGGCCGAGGGTCACGTGAAGGGCGGCGCGAAGAAGGTGGTGATCAGCG 316
WHA1_GAPDH 327 CTCCGGCGTCCGGCGGTGCCAAGACGATCGTGATGGGCGTGAACCAGCACGAGTACAACCCGGCGACGCACCACGTGGT 405
Cb_GAPDH 317 CTCCGGCGTCCGGCGGTGCCAAGACGATCGTGATGGGCGTGAACCAGCACGAGTACAACCCGGCGACGCACCACGTGGT 395
Ce_GAPDH 317 CGCCGGCGTCCGGCGGTGCCAAGACGATCGTGATGGGCGTGAACCAGCACGAGTACGATCCGGCCAAGCACCACATCGT 395
WHA1_GAPDH 406 GTCG 409
Cb_GAPDH 396 GTCG 399
Ce_GAPDH 396 GTCG 399
B
WHA1_ssrRNA 1 GGCGTTGACGGGAGCGGGGGATTAGGGTTCGATTCCGGAGAGGGAGCCTGAGAAATAGCTACCACTTCTACGGAGGGCA 79
Cb_ssrRNA 12 GGCGTTGACGGGAGCGGGGGATTAGGGTTCGATTCCGGAGAGGGAGCCTGAGAAATAGCTACCACTTCTACGGAGGGCA 90
Ce_ssrRNA 12 AGCGTTGACGGGAGCGGGGGATTAGGGTTCGATTCCGGAGAGGGAGCCTGAGAAATAGCTACCACTTCCACGGAGGGCA 90
WHA1_ssrRNA 80 GCAGGCGCGCAAATTGCCCAATGTCAAAACAAAACGATGAGGCAGCGAAAAGAAATAGAGTTGTCAGTCCATTTGGATT 158
Cb_ssrRNA 91 GCAGGCGCGCAAATTGCCCAATGTCAAAACAAAACGATGAGGCAGCGAAAAGAAATAGAGTTGTCAGTCCATTTGGATT 169
Ce_ssrRNA 91 GCAGGCGCGCAAATTGCCCAATGTCAAAACAAAACGATGAGGCAGCGAAAAGAAATAGAGCAGTCAGTCCATTTGGATT 169
WHA1_ssrRNA 159 GTCATTTCAATGGGGGATATTTAAACCCATC-CATATCGAGTAACAATTGGAGGACAAGTCTGGTGCCAGCACCCGCGG 236
Cb_ssrRNA 170 GTCATTTCAATGGGGGATATTTAAACCCATCCAATATCGAGTAACAATTGGAGGACAAGTCTGGTGCCAGCACCCGCGG 248
Ce_ssrRNA 170 GACTTTTCAATGGGGGATATTTAAACCCATCCAATATCGAGTAACAATTGGAGGACAAGTCTGGTGCCAGCACCCGCGG 248
WHA1_ssrRNA 237 TAATTCCAGCTCCAAAAGCGTATATTAATGCTGTTGCTGTTAAAGGGTTCGTAGTTGAACTGTGGGTTGTGTAGGTTTG 315
Cb_ssrRNA 249 TAATTCCAGCTCCAAAAGCGTATATTAATGCTGTTGCTGTTAAAGGGTTCGTAGTTGAACTGTGGGTTGTGTAGGTTTG 327
Ce_ssrRNA 249 TAATTCCAGCTCCAAAAGCGTATATTAATGCTGTTGCTGTTAAAGGGTTCGTAGTTGAACTGTGGGCTGTGTAGGTTTG 327
WHA1_ssrRNA 316 TTCCTGGTCGTCCCGTCCATGTCGGATTTGGTGGCCCAGGCCCTTGCAGCCCGTGAACATTCAAAGAAACAAGAAACAC 394
Cb_ssrRNA 328 TTCCTGGTCGTCCCGTCCATGTCGGATTTGGTGGCCCAGGCCCTTGCAGCCCGTGAACATTCAAAGAAACAAGAAACAC 406
Ce_ssrRNA 328 TTCCTGGTCGTCCCGTCCATGTCGGATTTGGTGGCCCAGGCCCTTGCAGCCCGTGAACATTCAAAGAAACAAGAAACAC 406
WHA1_ssrRNA 395 GGGAGTGGTTCCTTTCCTGATCTACGCATGTCATGCATGCCAGGGGGCGTCCGTGA 450
Cb_ssrRNA 407 GGGAGTGGTTCCTTTCCTGATCCACGCATGTCATGCATGCCAGGGGGCGTCCGTGA 462
Ce_ssrRNA 407 GGGAGTGGTTCCCTTCCTGATCTACGCATGTCATGCATGCCAGGGGGCGTCCGTGA 462
C
WHA1 46 AGTGTTCATATTTGTTTTACGTCATTATTATTTTTTTTATTGTATGTACATATTTTTAAAGCAATCGTTTTAATTATAT 124
08.076 1 AGTGTTCATATTTGTTTTACGTCATTATTATTTTTTTTATTGTATGTACATATTTTTAAAGCAATCGTTTTAATTATAT 79
CbombiBJ08.85 24 AGTGTTCATATTTGTTTTACGTCATTATTATTTTTTTTATTGTATGTACATATTTTTAAAGCAATCGTTTTAATTATAT 102
CbombiAK08.053 24 AGTGTTCATATTTGTTTTACGTCATTATTATTTTTTTTATTGTATGTGCATATTTTTAAAGCAATTGTTTTAATTATAT 102
CexpoekiBJ08.85 24 AGTACCCATATTTGTTTTACGTCATTATTGTTTTTTTTATTATATGTTCATATTTTTAAAGCAATTGTATTAATTATAT 102
CexpoekiAK08.209 24 AGCACCCATATTTGTTTTACGTCATTATTGTTTTTTTTATTATATGTCCATATTTTTAAAGCAATTGTATTAATTATAT 102
WHA1 125 TATTTGATACTCATATTTTAGTGTGGGCTGTTGGATTTGTTATTTATATTTTATTGTTGTAATAGGTTTTATAGGTTA 203
08.076 80 TATTTGATACTCATATTTTAGTGTGGGCTGTTGGATTTGTTATTTATATTTTATTGTTGTAATAGGTTTTATAGGTTA 158
CbombiBJ08.85 103 TATTTGATACTCATATTTTAGTGTGGGCTGTTGGATTTGTTATTTATATTTTATTGTTGTAATAGGTTTTATAGGTTA 181
CbombiAK08.053 103 TATTTGATACTCATATTTTAGTGTGGGCTGTTGGATTTGTTATTTATATTTTATTGTTGTAATAGGTTTTATAGGTTA 181
CexpoekiBJ08.85 103 TATTTGACACTCATATTTTAGTATGAACAGTCGGTTTTATAATATATATATTTATAGTTGTTATAGGTTTTATTGGATA 181
CexpoekiAK08.209 103 TATTTGACACTCATATTTTAGTATGAACAGTTGGTTTTATAATATATATATTTATAGTTGTTATAGGTTTTATTGGATA 181
WHA1 204 TGTTTTACCGTGTACAATGATGTCTTATTGAGGATTAACAGTTTTTAGTAATATTTTGGCCACTGTACCAGTTATTGGT 282
08.076 159 TGTTTTACCGTGTACAATGATGTCTTATTGAGGATTAACAGTTTTTAGTAATATTTTGGCCACTGTACCAGTTATTGGT 237
CbombiBJ08.85 182 TGTTTTACCGTGTACAATGATGTCTTATTGAGGATTAACAGTTTTTAGTAATATTTTGGCCACTGTACCAGTTATTGGT 260
CbombiAK08.053 182 TGTTTTACCATGTACAATGATGTCTTATTGAGGATTAACAGTTTTTAGTAATATTTTGGCCACTGTACCAGTTATTGGT 260
CexpoekiBJ08.85 182 TGTATTACCATGTACTATGATGTCGTATTGAGGTTTAACTGTTTTTAGTAATATTTTAGCAACAGTACCAGTTATTGGT 260
CexpoekiAK08.209 182 TGTATTACCATGTACTATGATGTCGTATTGAGGTTTAACTGTTTTTAGTAATATTTTAGCAACAGTGCCAGTTATTGGT 260
WHA1 283 TTATGATTGTGTTATTGAATTTGAGGAAGTGAATTTATTAATGATTTTACGTTACTGAAATTACATGTGTTGCATGTTT 361
08.076 238 TTATGATTGTGTTATTGAATTTGAGGAAGTGAATTTATTAATGATTTTACGTTACTGAAATTACATGTGTTGCATGTTT 316
CbombiBJ08.85 261 TTATGATTGTGTTATTGAATTTGAGGAAGTGAATTTATTAATGATTTTACGTTACTGAAATTACATGTGTTGCATGTTT 339
CbombiAK08.053 261 TTATGATTGTGTTATTGAATTTGAGGCAGTGAGTTTATTAATGATTTTACGTTATTGAAATTACATGTGTTGCATGTTT 339
CexpoekiBJ08.85 261 TTATGATTGTGTTATTGAATATGAGGTAGTGAATTTATTAATGATTTTACTTTATTAAAATTACATGTTTTACATGTTT 339
CexpoekiAK08.209 261 TTATGATTGTGTTATTGAATATGAGGTAGTGAATTTATTAATGATTTTACTTTATTAAAATTGCATGTTTTACATGTTT 339
WHA1 362 TATTGCCATTTGTTTTAATTTTAGTTATTGTAATGCATTTGTTTTGTTTACATTATTTTATGAGTTCAGATGGTTTT 438
08.076 317 TATTGCCATTTGTTTTAATTTTAGTTATTGTAATGCATTTGTTTTGTTTACATTATTTTATGAGTTCAGATGGTTTT 393
CbombiBJ08.85 340 TATTGCCATTTGTTTTAATTTTAGTTATTGTAATGCATTTGTTTTGTTTACATTATTTTATGAGTTCAGATGGTTTT 416
CbombiAK08.053 340 TATTACCATTTGTTTTAATTTTAGTTATTGTAATGCATTTGTTTTGTTTACATTATTTTATGAGTTCAGATGGATTT 416
CexpoekiBJ08.85 340 TATTGCCATTTGTATTGATTTTAATAATAATCATGCATTTATTTTGTTTACATTATTTTATGAGTTCAGACGGTTTT 416
CexpoekiAK08.209 340 TATTGCCATTTGTATTAATTTTAATAATAATCATGCATTTATTTTGTTTACATTATTTTATGAGTTCAGATGGTTTT 416

GFP

RFP

GFP-RFP-TD

Uninfected

A

B

C

GFP-*C. bombi*

D

E

F

G

RFP-*C. bombi*

H

I

J

K

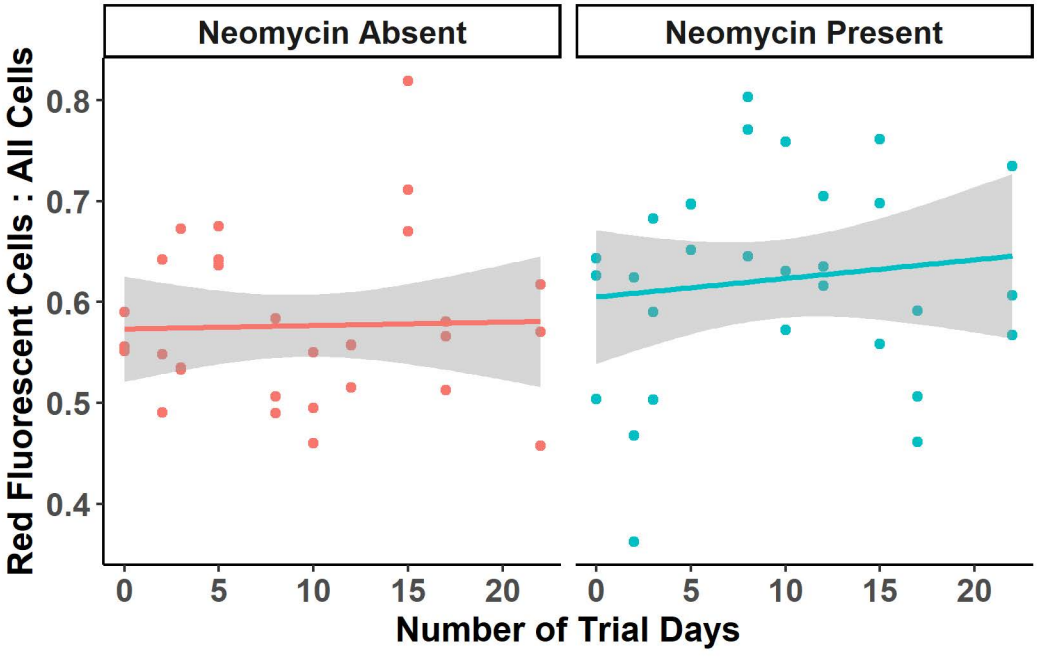
Neomycin Absent
Neomycin Present
Red Fluorescent Cells : All Cells
0.8
0.7
0.6
0.5
0.4
0
5
10
15
20
Number of Trial Days